

Increase in Width of the Giant Dipole Resonance in Hot Nuclei: Shape Change or Collisional Damping?

A. Bracco, F. Camera, M. Mattiuzzi, B. Million, and M. Pignanelli

*Dipartimento di Fisica, Università di Milano,
and Istituto Nazionale di Fisica Nucleare Sezione di Milano, via Celoria 16, 20133 Milano, Italy*

J. J. Gaardhøje, A. Maj,* T. Ramsøy,† T. Tveter,‡ and Z. Želazny,§

*The Niels Bohr Institute, Blegdamsvej 15-17, Copenhagen DK-2100 Ø, Denmark
(Received 29 November 1994)*

The strength function and the angular distribution of the high energy γ rays emitted by the giant dipole resonance (GDR) in hot rotating $^{109,110}\text{Sn}$ nuclei have been measured at temperature $T = 1.8$ MeV and at four values of the angular momentum I . The GDR width is ≈ 2 times larger than at $T = 0$ and increases by $\approx 20\%$ as I goes from 40 to $54\hbar$. The $a_2(E_\gamma)$ increases by a factor of ≈ 2 . Based on these two facts and on the comparison with theory we conclude that large deformations driven by I and combined with shape and orientation fluctuations are responsible for the measured increases. Collisional damping is constant and practically equal to the $T = 0$ case.

PACS numbers: 24.30.Cz, 23.20.Lv, 25.70.Gh, 27.60.+j

A central issue in the understanding of the width of the giant dipole resonance (GDR) in atomic nuclei at finite temperature is to separate the contributions from the different damping mechanisms so that their dependence on temperature and on rotational frequency can be studied.

The spreading of the strength of giant resonances is mainly due to two mechanisms. The first is the mixing of the correlated one particle one hole state with more complicated states lying at the same excitation energy. This is the collisional damping which is connected with the coupling of the giant vibrational modes to the small amplitude quantal fluctuations of the nuclear surface. Various predictions of the collisional damping width Γ^{\downarrow} exist. In Ref. [1], making use of the Vlasov equation, an increase of the width with temperature for Sn and Pb has been predicted. In Ref. [2], using the time dependent density matrix method, it has been found that the width of the GDR and of the giant quadrupole resonance (GQR) in ^{16}O and in ^{40}Ca is independent of temperature. This result is also found in Ref. [3] using the surface coupling model applied to the GDR in ^{90}Zr and ^{208}Pb . The additional coupling of the GDR to the fully mixed states describing the compound nucleus has also been found to be independent of temperature [4].

The second important mechanism at work in the breaking of the strength of the GDR is the coupling of the vibration to large amplitude fluctuations (shape fluctuations) of the nuclear surface that are induced by temperature. At finite temperature and rotational frequency the nucleus can be viewed as an ensemble of shapes with a distribution controlled by the Boltzmann factor [5,6]. An averaging of the GDR vibrations over the distribution of shapes is therefore necessary to predict the GDR width. This ensemble of shapes, at the temperature at which shell effects have vanished, depends strongly on the angular momentum, since the Coriolis and centrifugal forces make the

nucleus deform as an oblate liquid drop. While angular momentum induces large oblate equilibrium deformations, thermal fluctuations make the GDR sample large deformations far away from the equilibrium shape [7]. As a consequence, the GDR width, Γ_{GDR} , should increase.

In spite of the existence of a large body of systematics extending up to very high excitation energies (≈ 550 MeV) concerning the width of the GDR in the mass region $A \approx 110$ [8–14], the effects of the two damping mechanisms have never been clearly separated experimentally. The width increase observed in this mass region has been deduced from measurements of the high energy γ spectra associated to the entire spin distributions of the compound nucleus, distributions that were different for the variety of the reactions used. Consequently, the existing data contain both angular momentum and excitation energy contributions, although angular momentum effects were suggested to play a major role [14].

In the present Letter we report on measurements of the spectra and of the angular distribution of the high energy γ rays emitted in the decay of the giant dipole resonance from hot and rotating $^{109,110}\text{Sn}$ nuclei at $T \approx 1.8$ MeV and defined to four narrow intervals of the angular momentum of the compound nucleus. The purpose of the experiments has been to investigate in detail the influence of angular momentum on the measured width of the GDR in hot rotating nuclei. We show for the first time that the combined analysis of the strength function and of the $a_2(E_\gamma)$ coefficient of the angular distribution make it possible to extract information on the damping mechanism, namely on the collisional damping and on the shape effects induced by angular momentum and by thermal fluctuations.

The importance of a simultaneous study of the GDR line shape and $a_2(E_\gamma)$ is illustrated in Fig. 1. A broadening of the GDR width Γ_{GDR} can be due either to an

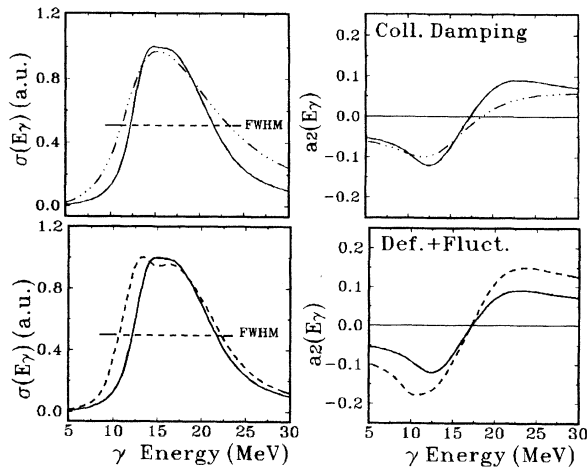


FIG. 1. Strength function (left) and $a_2(E_\gamma)$ (right) calculated with the adiabatic thermal fluctuation model at $T = 2$ MeV. The calculations in the top part use the intrinsic width (see text) $\Gamma_0^\dagger = 5$ MeV (full drawn lines) and $\Gamma_0^\dagger = 6$ MeV (dot-dashed lines) and the same rotational frequency $\omega = 1.0$ MeV. The calculations in the bottom part both use $\Gamma_0^\dagger = 5$ MeV and $\omega = 1.0$ MeV (full drawn lines) and $\omega = 1.25$ MeV (dashed lines). Note that the FWHM (dashed lines) is the same.

increase of the collisional damping width or to an increase of the size of the nuclear deformation. In this example we have considered an increase in Γ_{GDR} of 1 MeV. If that increase is due to an increase of the collisional damping width (dot-dashed curve in the top row of Fig. 1) the associated $a_2(E_\gamma)$ is almost unchanged. If, on the contrary, Γ_{GDR} increases because the deformation to which the GDR couples is larger, the absolute value of the associated $a_2(E_\gamma)$ increases (calculations shown with the dashed lines in the bottom row of Fig. 1). The strength function and the $a_2(E_\gamma)$ were calculated with the thermal fluctuation model of shape and orientation [5,6] in the adiabatic limit. In this procedure the averaging over the shape distributions is made in terms of the Boltzmann factors $\exp[-F(T, \omega, \beta, \gamma)/T]$ (F is the free energy, T the temperature, ω the rotational frequency, and β, γ the quadrupole deformation parameters). The centroids of the GDR components are given by the Hill-Wheeler parametrization and their widths scaled by $\Gamma^\dagger = \Gamma_0^\dagger (E_{\text{GDR}}/E_0)^\delta$ using $E_0 = 15.5$ MeV, $\delta = 1.9$. The width increase of the GDR strength function was obtained, in the top part, by increasing the collisional damping width by changing the value of Γ_0^\dagger from 5 to 6 MeV, while in the bottom case by increasing ω , since at $T = 2$ MeV shell effects have vanished and consequently faster rotations induce larger deformations.

The hot and rotating $^{110,109}\text{Sn}$ nuclei were formed in the fusion reactions $^{48}\text{Ti} + ^{62,61}\text{Ni}$ at beam energies 223 and 203 MeV. The beams were produced by the tandem + booster accelerators of the Tandem Laboratory of the Niels Bohr Institute. Target thicknesses were 1 mg/cm². High and low energy γ rays were detected with the HECTOR

array [15]. The latter consists of 8 large volume BaF₂ crystals positioned at different angles ($\pm 60^\circ$, $\pm 90^\circ$, $\pm 120^\circ$, and $\pm 160^\circ$) and 38 smaller BaF₂ used as multiplicity filters. Neutron and γ separation was obtained by measuring time of flights from the target. Gain shifts were monitored to better than 0.2% with a light-emitting diode system. The energy calibration was done with the 15.1 MeV γ rays from the $\text{D}(^{11}\text{B}, n\gamma)^{12}\text{C}^*$ reaction.

The response function of the multiplicity filter was determined as in Ref. [16]. An absolute efficiency of 70% was measured for the 1.172 MeV line from a ^{60}Co source. The electronic threshold of the detectors was set at ~ 250 keV. The measured cross talk between two elements was 12%. The conversion between the measured coincidence fold F_γ (the number of measured coincident γ rays of low energy in one event) and the multiplicity M_γ (the number of γ rays emitted in the reactions) was established, making use of the measured response matrix $S(M_\gamma, F_\gamma)$ and assuming that the multiplicity distribution following the fusion reaction is given by $f(M_\gamma) = M_\gamma / \{1 + \exp[(M_\gamma - M_0)/a]\}$. The maximum of the multiplicity M_0 and the diffuseness a were obtained as the best fitting values to the expressions $\sum S(M_\gamma, F_\gamma) f(M_\gamma) = f_{\text{exp}}(F_\gamma)$ where $f_{\text{exp}}(F_\gamma)$ is the measured multiplicity spectrum in the region $F_\gamma > 9$. The multiplicity distribution associated to each fold is $P(M_\gamma) = S(M_\gamma, F_\gamma) f(M_\gamma)$, with $M_0 = 23$ and $a = 2$ as it results from the fit.

The conversion from M_γ to I was done assuming $I = 2M_\gamma + K$. In this expression $K = 6$ takes into account the angular momentum removed by statistical γ rays, particle emission, and by the γ rays below the trigger threshold.

The total spectra of $^{110,109}\text{Sn}$ associated with the entire distribution of folds larger than 9 are shown in Fig. 2. These spectra were obtained rejecting the very high energy region of the sum energy spectrum measured with the multiplicity filter. In this way it was possible to eliminate background from cosmic rays. The full drawn lines are best fit statistical model calculations, using the code CASCADE [17], made for excitation energies $E^* = 80$ for ^{109}Sn and 92 MeV for ^{110}Sn . They correspond to $\Gamma_{\text{GDR}} = 11.8 \pm 0.6$ and $E_{\text{GDR}} = 14.9 \pm 0.5$ MeV for ^{110}Sn and $\Gamma_{\text{GDR}} = 11.4 \pm 0.6$ and $E_{\text{GDR}} = 15.7 \pm 0.5$ MeV for ^{109}Sn . The two values of the centroid differ more than the expected value of 1%. The dipole strength was assumed to exhaust 100% of the energy weighted sum rule (EWSR). The level density parameter a was $A/8$ in accord with most previous analyses in this E^* region.

The high energy γ -ray data have been also sorted gating on different F_γ . The values of initial T , of the average T and I , and of the FWHM of the I distributions are listed in Table I with the GDR parameters.

The measured γ -ray spectra associated with the selected I intervals were also fitted in the GDR region with statistical model calculations. The centroid and the width values were obtained from the best fit to the data using

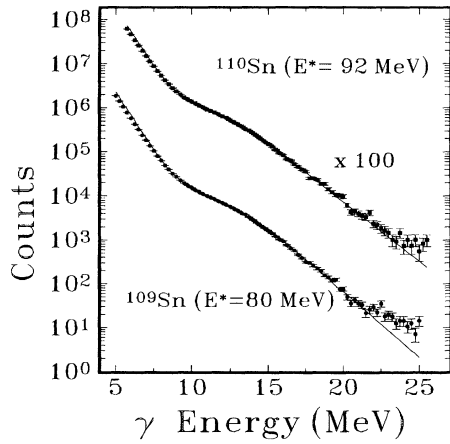


FIG. 2. Experimental spectra for $^{110}\text{Sn}^*$ at $E^* = 92$ MeV (top) and $^{109}\text{Sn}^*$ at $E^* = 80$ MeV (bottom) associated to coincidence folds $F_\gamma > 9$ ($\langle I \rangle = 45\hbar$ and $\text{FWHM}_I = 24\hbar$.) The full drawn lines are best fit statistical model calculations with $E_{\text{GDR}} = 14.9$ MeV, $\Gamma_{\text{GDR}} = 11.7$ MeV for ^{110}Sn and to $E_{\text{GDR}} = 15.7$ MeV, $\Gamma_{\text{GDR}} = 11.4$ MeV for ^{109}Sn .

a χ^2 minimization procedure. Because of the exponential nature of the spectra the χ^2 of this fit is dominated by the low energy part and is relatively insensitive to the GDR region; consequently, the best fitting GDR parameters were chosen to be those minimizing the χ^2 divided by the number of counts. For the fusion cross section as a function of I , the measured distributions were used. The error of the GDR parameters reported in Table I include the statistical error and the uncertainties related to the spin assignment and to the excitation energy.

The data associated to restricted regions of I are shown together with the statistical model calculations in Fig. 3 (left column). In order to display spectra on a linear scale to emphasize the GDR region the quantity $F(E_\gamma)Y_\gamma^{\text{exp}}(E_\gamma)/Y_\gamma^{\text{cal}}(E_\gamma)$ was plotted. $Y_\gamma^{\text{exp}}(E_\gamma)$ is the experimental spectrum and $Y_\gamma^{\text{cal}}(E_\gamma)$ the best fit calculated spectrum, corresponding to the single Lorentzian function $F(E_\gamma)$. For the data at high I a fit with two Lorentzians was made but we could not infer unambiguously the type of deformation (oblate or prolate) and thus compute the

TABLE I. The results of the statistical model analysis of the spectra of the nuclei given in the first column. The initial temperature T , the average T (both in MeV), and angular momentum I (in \hbar) are given in columns 2, 3, and 4. The values of the centroid and of the width of the best fit statistical model calculations are listed in columns 5 and 6 (both in MeV). The errors in these data are 0.500 and 0.600 MeV, respectively. The FWHM (in \hbar) of the I distributions are in column 7. The FWHM of the T distribution is 0.3 MeV (+0.1 MeV, -0.2 MeV). The notation (a), (b), (c), and (d) is used in Fig. 3.

Nucleus	T	$\langle T \rangle$	$\langle I \rangle$	E_{GDR}	Γ_{GDR}	FWHM_I
^{109}Sn (a)	1.79	1.6	40	15.7	10.8	18
^{110}Sn (b)	1.96	1.8	44	15.0	11.7	16
^{109}Sn (c)	1.57	1.4	49	15.6	11.4	16
^{110}Sn (d)	1.74	1.6	54	14.7	12.8	14

associated $a_2(E_\gamma)$. However, since deformation affects the total GDR width, a fit with one Lorentzian does not necessarily imply a spherical nucleus, as one can see from the measured $a_2(E_\gamma)$ that are different than zero.

The measurements of the $a_2(E_\gamma)$ are shown in the right part of Fig. 3. The $a_2(E_\gamma)$ distributions were obtained by fitting the spectra measured at different angles to the function $N(E_\gamma, \theta) = N_0(E_\gamma)[1 + a_2(E_\gamma)P_2(\cos\theta)]$, where $P_2(\cos\theta)$ is the Legendre polynomial in the polar angle θ between the γ ray and the beam direction. The spectra at the different angles have been normalized at $E_\gamma = 6-7$ MeV.

This measurement of dependence of the GDR width on angular momentum at rather fixed temperature ($T = 1.6-2.0$ MeV) shows that by changing I from $40\hbar$ to $55\hbar$ the width increases by ≈ 2 MeV. This result confirms

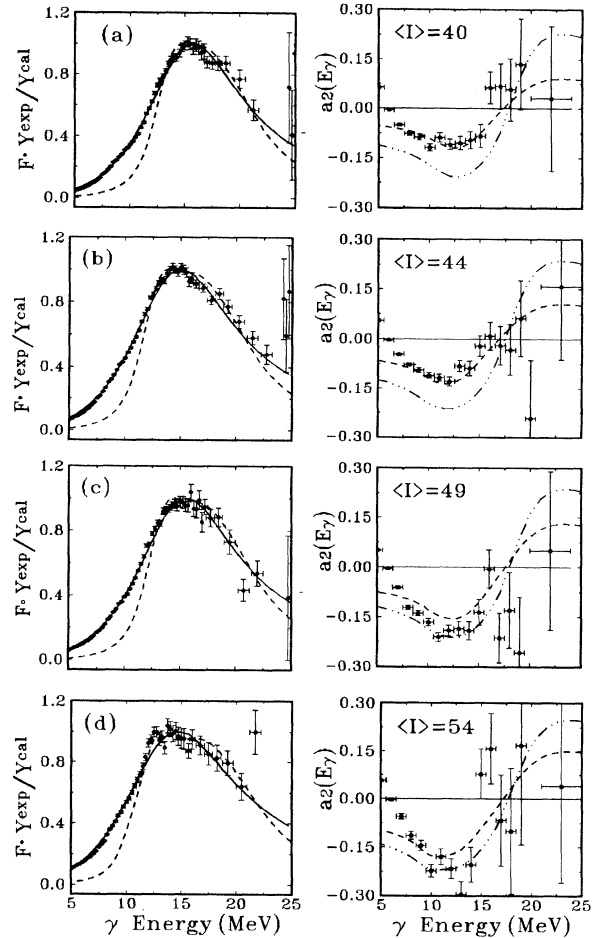


FIG. 3. Measured strength functions and $a_2(E_\gamma)$ for four different angular momenta. In the left part of the figure the quantity $F(E_\gamma)Y_\gamma^{\text{exp}}(E_\gamma)/Y_\gamma^{\text{cal}}(E_\gamma)$ (see text) is plotted. The full drawn lines correspond to the best fitting single component Lorentzian functions. The values of the measured GDR parameters are in Table I. The dashed lines are calculations with the model of thermal fluctuations of shape and orientation in the adiabatic limit. The dot-dashed lines include only shape fluctuations.

previous indications that angular momentum effects are to a very large extent responsible for the observed width increase. The magnitude of the measured $a_2(E_\gamma)$ also increases with angular momentum in a more pronounced way. To understand this stronger effect in the $a_2(E_\gamma)$ it is important to recall that, contrary to the strength function, the angular distribution depends also on the nuclear orientation and on its fluctuations, which are expected to decrease as angular momentum increases.

Based on the discussion made in connection with Fig. 1, this combined measurement of the two GDR observables indicates that the collisional damping width Γ^l does not change and that the measured increase of the GDR width Γ_{GDR} is mainly caused by the coupling of the dipole vibration to deformations that are largest at higher angular momenta.

To make this discussion more quantitative we compare the data to predictions obtained with the model of thermal fluctuations of shape and orientation in the adiabatic limit. The calculations were made for the ensembles of (T, ω) values corresponding to the (E^*, I) regions relevant for the present cases. Γ_0^l was chosen equal to 5 MeV. Two sets of calculations were made, one including only shape fluctuations and the other both shape and orientation fluctuations (dot-dashed and dashed lines in Fig. 3, respectively). While the two sets coincide in the case of the strength function (which does not depend on orientation), they are different in the case of the $a_2(E_\gamma)$, although the difference does not vary appreciably in the considered I interval. The calculated strength functions, normalized to the data (in a.u.) in the centroid region, are slightly narrower than the measured ones, although the relative increase with angular momentum is reasonably well reproduced. In contrast, the increase of the magnitude of the $a_2(E_\gamma)$ is not very well predicted by the calculations including shape and orientation fluctuations and the data associated to the highest spin are better reproduced by calculations including only shape fluctuations, suggesting that either the fluctuations in orientation are overestimated at high angular momenta or the collisional damping width has a smaller value than the one used. This last possibility would lead to a smaller GDR width and, therefore, would be in disagreement with the spectra. Consequently, a sensible conclusion is that there is more averaging in the adiabatic model than necessary at high rotational frequency and that perhaps non-Lorentzian strength functions could improve the agreement with the spectra in the low energy region (8–10 MeV). This last idea is supported by recent calculations of collisional damping of the GDR in Sn leading to a strength function that is not Lorentzian and with some extra strength at low energies [18].

In summary, the strength function and the angular distribution of the γ rays from the GDR damping were measured for $^{110,109}\text{Sn}$ at $T \approx 1.8$ MeV and at four values of I . A width increase of the order of 2 MeV was found in the

angular momentum interval 40–55 \hbar . In the same interval the absolute value of the $a_2(E_\gamma)$ also increases. These two facts demonstrate that the width increase is mainly due to the effect of larger deformations induced by angular momentum and that the collisional damping width does not change significantly. The comparison with calculations including thermal fluctuations supports this idea but also suggests reduced orientation fluctuations at high angular momenta. It would be interesting to perform such exclusive measurements of the two GDR observables also at higher temperatures extending up to the region of very high excitation energies ($E^* \geq 300$ MeV) where a quenching of the γ emission was found and recently confirmed [19]. This will allow us to map the shapes of very hot nuclei and provide detailed tests of new models for the damping of collective excitations in hot and rotating nuclei.

The support of the INFN, the Danish Natural Science Research Council, and the Carlsberg Foundation is acknowledged. A special thanks to E. W. Ormand for letting us use his code for thermal fluctuation calculations.

*Present address: Niewodniczański Institute of Nuclear Physics, Cracow, Poland.

†Present address: Radiation Protection Institute, Oslo, Norway.

‡Present address: Department of Physics, Oslo University, Box 1048 Blindern, N-0316 Oslo, Norway.

§Present address: Department of Physics, Warsaw University, Warsaw, Poland.

- [1] A. Smerzi *et al.*, Phys. Rev. C **44**, R1713 (1991); Phys. Lett. B **320**, 216 (1994).
- [2] F. V. De Blasio *et al.*, Phys. Rev. Lett. **68**, 1663 (1992).
- [3] P. F. Bortignon *et al.*, Nucl. Phys. **A460**, 149 (1986).
- [4] B. Lauritzen *et al.* (to be published); V. G. Zelevinsky *et al.*, Report No. NBI-93-45 (to be published).
- [5] E. W. Ormand *et al.*, Phys. Rev. Lett. **64**, 2254 (1990); **69**, 2905 (1992).
- [6] Y. Alhassid and B. Bush, Phys. Rev. Lett. **65**, 2527 (1990); Nucl. Phys. **A514**, 434 (1990); **A531**, 1 (1991).
- [7] F. Camera *et al.*, Nucl. Phys. **A572**, 401 (1994).
- [8] J. J. Gaardhøje, Annu. Rev. Nucl. Part. Sci. **42**, 483 (1992), and references therein.
- [9] K. Snover, Annu. Rev. Nucl. Part. Sci. **36**, 545 (1986).
- [10] J. J. Gaardhøje, Phys. Rev. Lett. **56**, 1783 (1986).
- [11] D. R. Chakrabarty *et al.*, Phys. Rev. C **36**, 1886 (1987).
- [12] A. Bracco *et al.*, Phys. Rev. Lett. **62**, 2080 (1989).
- [13] H. J. Hofmann, Nucl. Phys. **A569**, 301 (1994).
- [14] F. Camera *et al.*, Phys. Lett. B **293**, 18 (1992).
- [15] A. Maj *et al.*, Nucl. Phys. **A571**, 185 (1994).
- [16] M. Jäskeläinen *et al.*, Nucl. Instrum. Methods **207**, 385 (1983).
- [17] F. Pühlhofer, Nucl. Phys. **A280**, 267 (1977).
- [18] P. F. Bortignon *et al.*, Nucl. Phys. A (to be published).
- [19] J. H. Le Faou *et al.*, Phys. Rev. Lett. **72**, 3321 (1994).